

AN ANALOGUE OPTICAL LINK AT LIQUID ARGON TEMPERATURE

B. Dinkespiler, M. Jevaud, E. Monnier, C. Olivetto, S. Tisserant

Centre de Physique des Particules de Marseille, CPPM
IN2P3 et Université d'Aix Marseille II, Marseille, France

J.P. Coulon

Laboratoire de l'accélérateur linéaire, LAL
IN2P3-CNRS, Orsay, France

L.O. Eek, B. Lund-Jensen, J. Söderqvist

Royal Institute of Technology, KTH
Physics dept. Frescati, Stockholm, Sweden

Abstract

We present a feasibility study of an analogue optical link for the readout of an ATLAS presampler working in liquid argon. The specifications for such a link are given and the characteristics and performance of its various required components are described. A prototype is presented and its behaviour is briefly analysed. The conclusions of this study are that an analogue optical link with a maximum signal to noise ratio of 2000 and a differential non-linearity of 4% is working in liquid argon, and that a dynamic range of 5000 with a non-linearity below 2% seems reachable in a near future.

Figure 1: *Basic diagram of the optical link*

2 Specifications

First of all the link has to be reliable over the full expected 10 years of running at ATLAS. The desired link has to transmit signals over less than 100 metres. The required dynamic range is 5000 for a minimum-signal to noise ratio of one (or 1000 for a S_{min}/N of 5), with a linearity better than 2%. The bandwidth of the link has to be 50 MHz.

Apart from the electrical characteristics, the high level of radiation at LHC requires the link to withstand a radiation level of roughly 10^{14} neutrons/cm² and 1 Mrad, integrated over 10 years. We pursue a programme of irradiation tests to evaluate the radiation hardness of LEDs and optical fibres. Results from this on-going programme are reported in [1]. The emitting part located in the cryostat has to work in liquid argon at 89° K, which also means that the power dissipation needs to be kept low (≤ 20 mW/channel). Finally, the large number of channels (roughly 30,000) for the presampler detector implies a low cost link with as many integrated parts as possible.

3 Description of the link

We concluded that the link that best matches the above criteria should be analogue and have a light emitting diode (LED) as emitter and a PIN photodiode as receiver. The design of the full chain is sketched in figure 1. In the following sections each of the main components of the link are presented.

3.1 Emitter

The purpose of the emitter is to act as an electrical to optical converter for the front end electronic signal, which has a typical range from 0.0 to 2.5 V over a 50 Ω impedance. We decided to use a Light Emitting Diode (LED) as emitter. Although in principle a laser diode can achieve a higher dynamic range, a LED is cheaper, more robust, insensitive to reflections, and behaves better both at cold temperature and in high radiation environments. Moreover, LEDs are easier to make, to test and to handle.

We have concentrated on Aluminium Gallium Arsenide LEDs (crystal structure $\text{Al}_x\text{Ga}_{1-x}\text{As}$) which emit light at 850 nm wavelength. AlGaAs LEDs are surface emitting, hence more powerful and cheaper than InGaAsP diodes which are edge emitting. Moreover, using AlGaAs LEDs allows for a possible future integration with GaAs front end electronics.

In addition, InP (1300 nm) has not proven to be superior to GaAs regarding radiation hardness [1], and has the disadvantage of lower optical output and sensitivity to electrical discharges.

Although we think we can achieve an optical link that meets all the different requirements working at 850 nm wavelength, we will be open to investigate new high-performance components appearing on the market, even if they work at other wavelengths.

Parameter	Symbol	Min	Typ	Max	Units	Test Conditions
Fibre coupled power	P_o	50	70		μW	$I_F = 100\text{mA}$, 50/125 μm 0.20 NA fibre
Forward voltage	V_F		1.85	2.20	V	$I_F = 100\text{mA}$
Reverse voltage	BVR	1.0	5.0		V	$I_R = 10\mu\text{A}$
Peak wavelength	λ_P		850		nm	$I_F = 100\text{mA}$ DC
Spectral bandwidth	$\Delta\lambda$		60		nm	$I_F = 100\text{mA}$ DC
Response time					ns	1V prebias, 100mA peak
$T = 25^\circ\text{C}$, 10-90%	t_r		4	8		
$T = 25^\circ\text{C}$, 90-10%	t_r		6	10		
Analogue bandwidth	BWE		85		MHz	$I_F = 100\text{mA}$ DC, sinusoidal modulation
Temperature coefficient	$\Delta P_o / \Delta T$		-0.03		$\text{dB}/^\circ\text{C}$	$I_F = 100\text{mA}$ (over 25 to 125 $^\circ$)
Series resistance	r_s		4.0		Ω	DC
Capacitance	C		70		pF	$V_R = 0\text{V}$, $f = 1\text{MHz}$

Table 1: Main characteristics of the HFE4050 diode from Honeywell data sheets

Several diodes from different suppliers¹⁾ have been tested both at room temperature (to compare to the supplier's specifications) and at liquid nitrogen temperature (77°K, close to the operation temperature in liquid argon temperature). Some of the specifications of the most promising one (HFE4050) are given in table 1.

To select a diode fulfilling our specifications, several characteristics have been studied. The relation between input voltage and input current, giving the working range of the diode, is one of

¹⁾ Honeywell (HFE 4050-014), ABB HAFO (1A184, 1A314, 1A362), Laser Diodes Inc. (IRE331-005), Hewlett Packard (HBFR 1404-05)

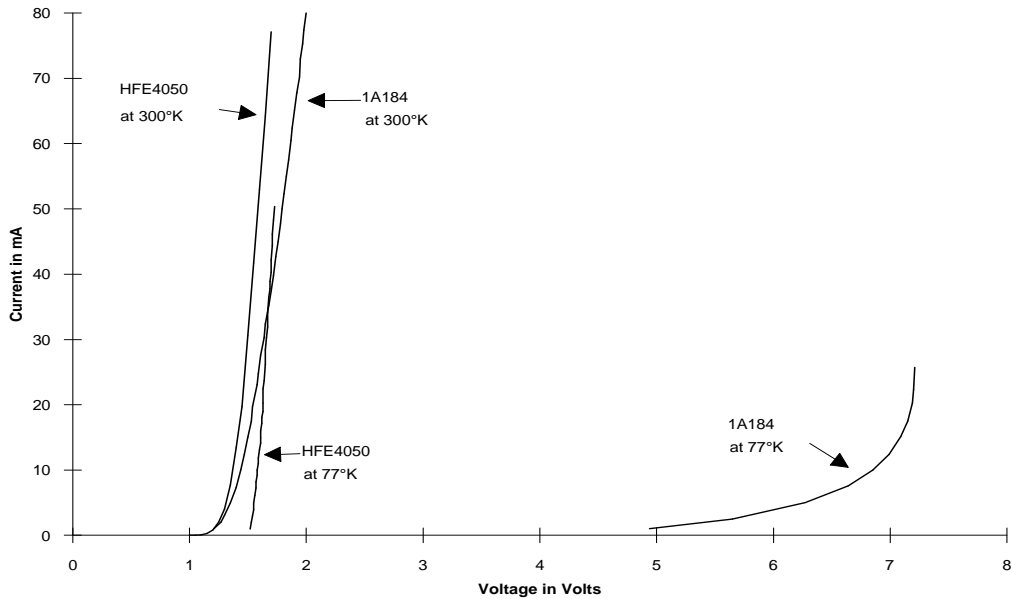


Figure 2: Voltage versus input current for several diode types and different working temperatures

them. This measurement is made by using a precise static voltage power supply²⁾ and by measuring the corresponding input current. In figure 2 are shown the resulting plots for two different diodes at room and liquid nitrogen ($77^{\circ}K$) temperatures. The curve for the HFE4050 shifts only slightly going to the cold temperature, whereas the 1A184 changes so drastically that it is not usable in the cold. It should be noted, however, that the 1A184 was not designed for operation at low temperatures. Its behaviour can be explained by its high level of Al content in the crystal which, at low temperatures, gives rise to so called DX donor states in the bandgap reducing the light output [2]. A later prototype, 1A362, from the same supplier, optimised for low temperature, does not exhibit this problem. These measurements point out the difficulties that can occur in using LEDs in cold environment.

One would like to keep the linearity and dynamic range as high as possible at the same time as the power dissipation should be minimised. In other words, a compromise has to be made between the largest linear working range and the smallest static voltage to current point. (To obtain dynamic linearity it is necessary to bias a LED with a static current, which should be as small as possible).

Measuring the voltage to current relation allows for a first selection among various diodes, but also measurements of the optical properties are needed to make a final choice.

The light yield, the dynamic range and the non-linearity of a diode must be studied, which means measuring the optical output versus the input current. This can be done either in static mode or in pulsed mode. The static test is easier to handle but, due to the risk of overheating, it does not permit as large a coverage of the dynamic range (additional non-linearity introduced at high input currents) as in the pulsed mode. Anyhow, a static input current of up to 50 mA can be

²⁾ Rhode Schwartz NGPT35

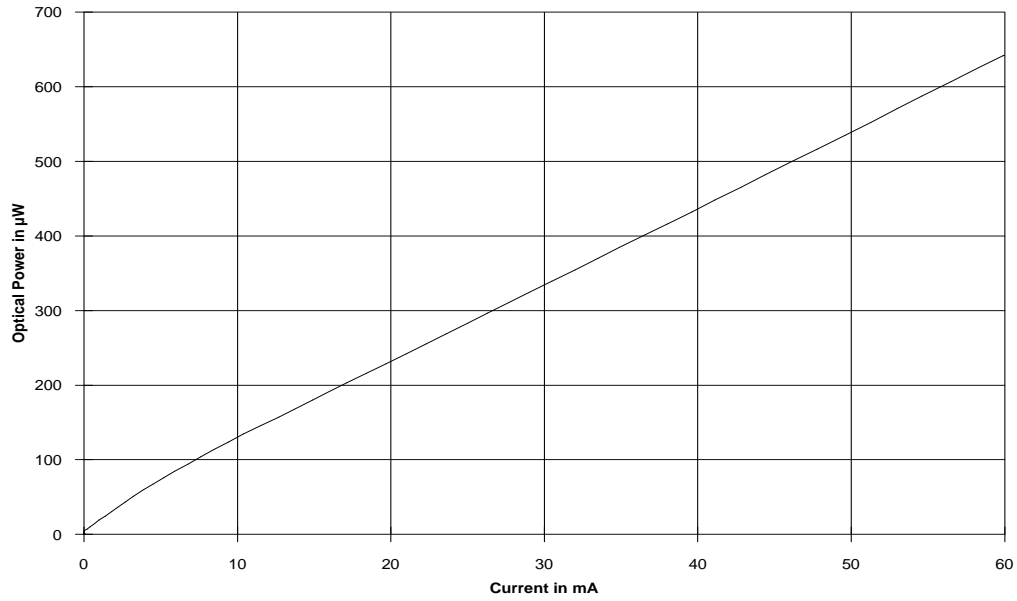


Figure 3: *Optical output power versus static input current at 77° K for a HFE4050 diode*

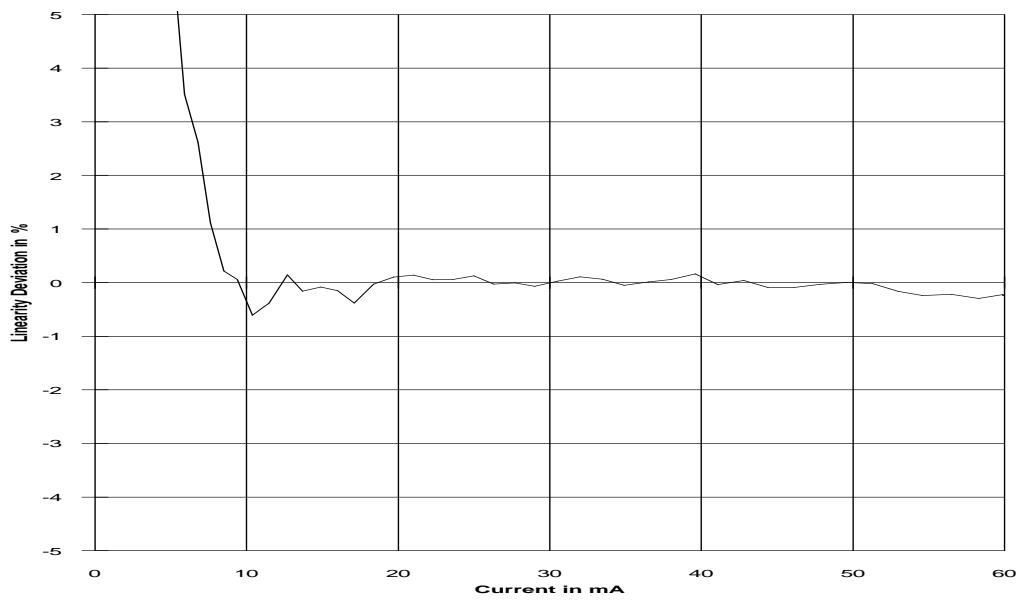


Figure 4: *Differential non-linearity for a HFE4050 diode at 77° K*

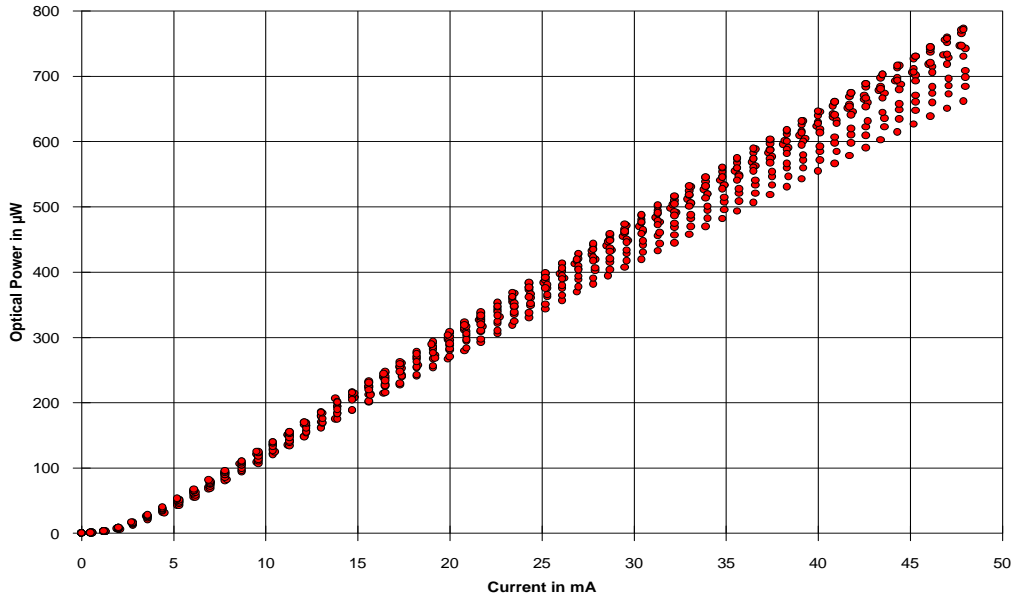


Figure 5: *Dispersion of the output power versus static forward current for several HFE4050 diodes at room temperature*

used. In the static test we measured the optical power³⁾ at the end of five metres of a 200 μm core fibre connected to a LED, as a function of the static input current sent through the LED. The light output power versus input current is given in figure 3 for the HFE4050 diode.

The linked differential non-linearity extracted from a linear fit is presented in figure 4. The choice of a bias point at 10 mA allows for a linear excursion of at least 50 mA with a non-linearity better than 2%. The corresponding polarisation voltage of 1.6 V, see figure 2, leads to a power dissipation of 16 mW from the LED alone, which is slightly too high with respect to the specifications but acceptable for our prototype.

Other diodes, using multiple quantum well techniques, have shown [3] bias points leading to a few mW power dissipation. These components look promising since they work well both at room and cold temperature and exhibit a good radiation hardness [3]. They will be tested in the near future.

Figure 5 shows the optical power versus static input current at room temperature for several samples of the same type of diode (HFE4050) from the same production batch. The dispersion in light output is below 10% (with less than 10% of the diodes out of specification) and the average ratio of light output to input current for the system of LED and fibre is 0.015 mW/mA. The ratio at liquid nitrogen temperature is (see figure 3) of the order of 0.01 mW/mA.

The static test allows for a quick overview of the main features of a diode but does not give the complete characteristics. Thus, in order to test a diode under working conditions, and to cover the complete dynamic range, AC tests were carried out, using a current pulse generator⁴⁾ to send a

³⁾ Power meter HP8252 from Hewlett Packard

⁴⁾ ILX LDP3811

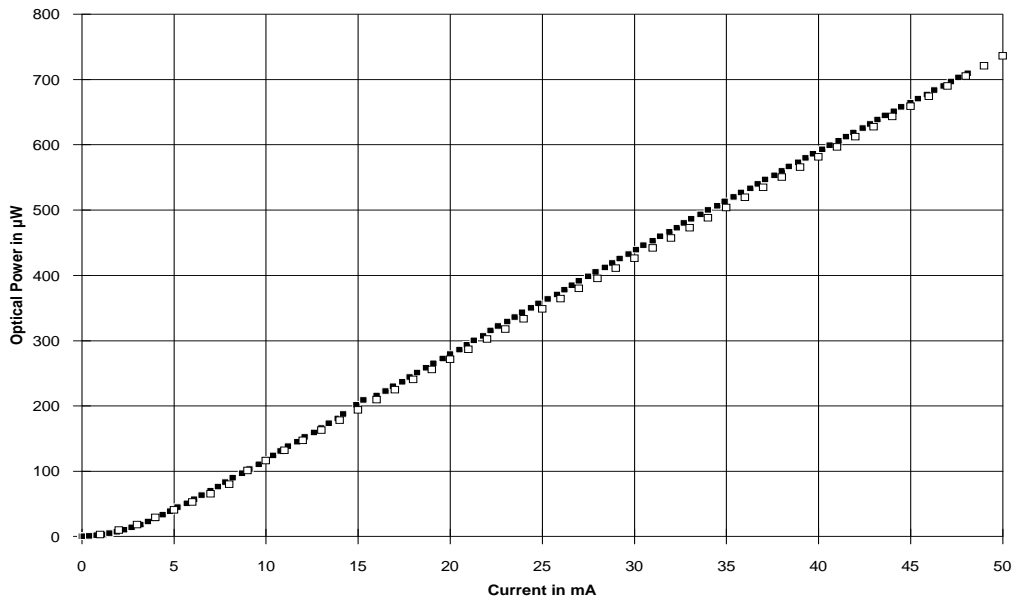


Figure 6: *Dynamic and static behaviour of a HFE4050 diode at room temperature normalised to the same optical output to cope with the uncertainties on the PIN+transimpedance gain*

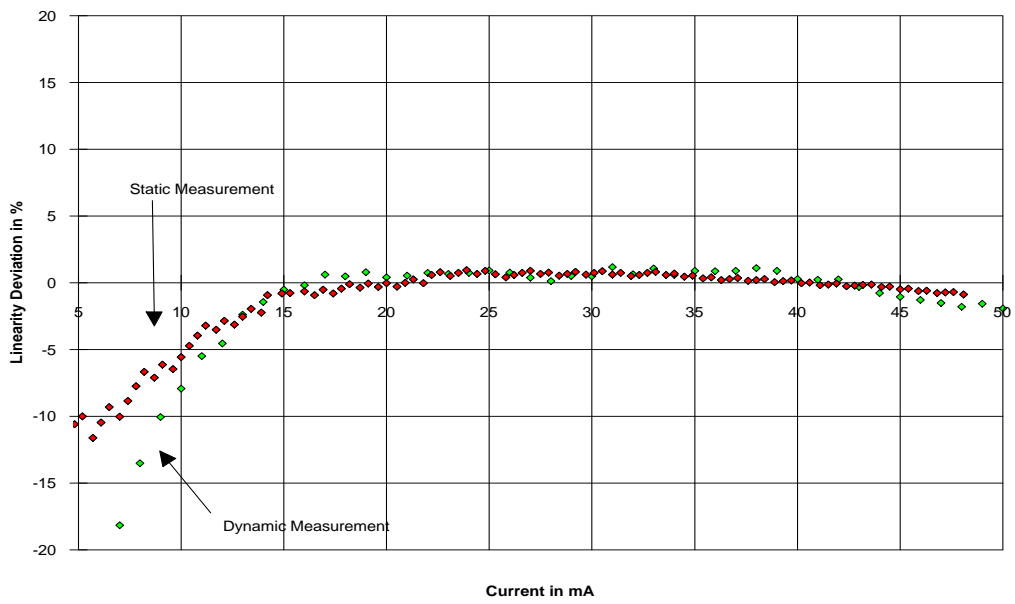


Figure 7: *Non-linearity of the dynamic and static behaviour of the HFE4050 diode at room temperature*

Figure 8: *Scheme of the dynamic test*

variable current pulse to the diode (with no bias current applied for intrinsic technical reason). The optical signal was transmitted, through five metres of 200 μm core fibre, to a PIN diode coupled to a transimpedance amplifier whose output signal was read by an oscilloscope and recorded by a computer. The setup can be seen in figure 8. Figures 6 and 7 show the dynamic excursion of the HFE4050 diode and the corresponding differential non-linearity. One can see that applying a 10 mA bias current and a forward pulse current of 50 mA to this LED gives an optical pulse of roughly 700 μW at the end of the 200 μm core fibre. Using the responsivity of the PIN diode (typically 0.5 A/W at 850 nm) and the gain of the transimpedance amplifier (given by the feedback resistor, see section 3.6) one can translate the output voltage into optical power, as indicated in figure 6, allowing for a direct comparison with the static measurements. (Since we have not yet precisely determined the conversion factors for the dynamic plot in figure 6 it was normalised to the same optical output as the static plot). A similar behaviour of the diode for static and dynamic measurements can be seen, which justifies the use of the static mode for a quick test. One of the disadvantages of the dynamic test, as compared to the static one, is that PIN diodes and additional amplifiers are needed, which are not easily calibrated.

The noise of a LED is negligible compared to the one of the front end electronics. The noise and the common behaviour of all parts of the prototype link is discussed in section 4.

Our study concludes that several commercial LEDs can fulfil our specifications.

3.2 Connectors

There are several different types of fibre-optical connectors commercially available, like FC, ST and SMA. For laboratory measurements and for the link prototype we have chosen the ST type, which is more robust, reliable and stable than the SMA, less expensive than the FC, and easy to

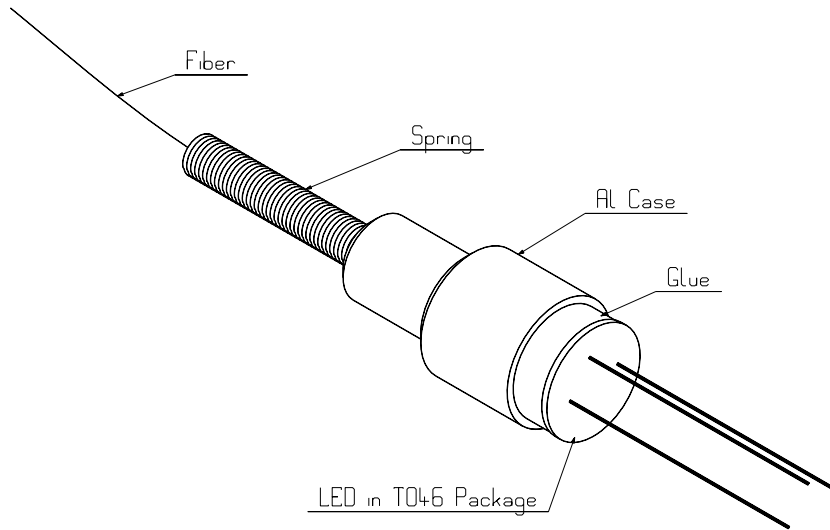


Figure 11: *Design of the pigtail packaging*

mount. We have used connectors with ceramic or metallic ferrule and a $250\ \mu\text{m}$ capillar hole. The connectors can be used to connect fibres to fibres or fibres to optical components.

We have tested the ST connector at room temperature and at liquid nitrogen temperature. The induced loss is smaller than 0.1 dB in both cases. No problems are expected in high radiation environments, a fact which has been confirmed in our irradiation studies of LEDs and fibres.

3.3 Fibres

Our choice is to use step index profile fibres with a pure silica core, a fluorine-doped silica cladding and a polyimide primary coating (typically $200/220/245\ \mu\text{m}$ outer diameter).

Using a pure silica fibre (core and cladding) is motivated by its radiation hardness to neutrons and gamma and its intrinsic good behaviour in the cold (to be compared to fibers with hard polymer cladding). Polyimide (unlike other kind of polymer) is a suitable material for the coating since its thermal expansion coefficient is similar to that of silica, preventing the occurrence, in the cold, of stress-induced losses in the fibres. It has also a good behaviour in the radiation and do not pollute the liquid argon. The typical attenuation factor for such silica/silica fibres is of the order of $4\ \text{dB}/\text{km}$ and the typical bandwidth is $15\ \text{MHz} \times \text{km}$ (150 MHz for 100m). Different types from various manufacturers⁵⁾ have been tested in the cold and in high neutron radiation environment, proving our choice [1] to be a suitable one. But, we will continue our tests and will investigate in a near future the possibility to use hard polymer cladding fibers.

3.4 Diode to fibre coupling

It is important to achieve a good optical coupling of the fibre to the LED. Therefore, LEDs are usually equipped with a lens system to increase the power coupled into the fibre by changing the spatial profile of the emitted light. A diode with a single collimating ball lens, such as the

⁵⁾ CeramOptec, Fujikura, Polymicro, Spectran, 3M

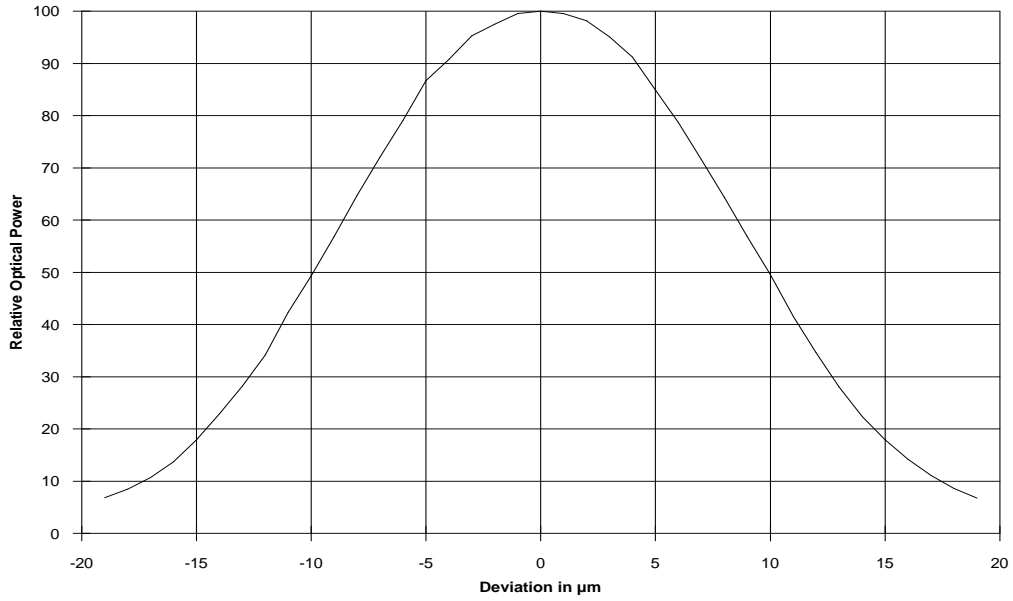


Figure 9: *Optical output power versus radial displacement with respect to the diode emitting axis*

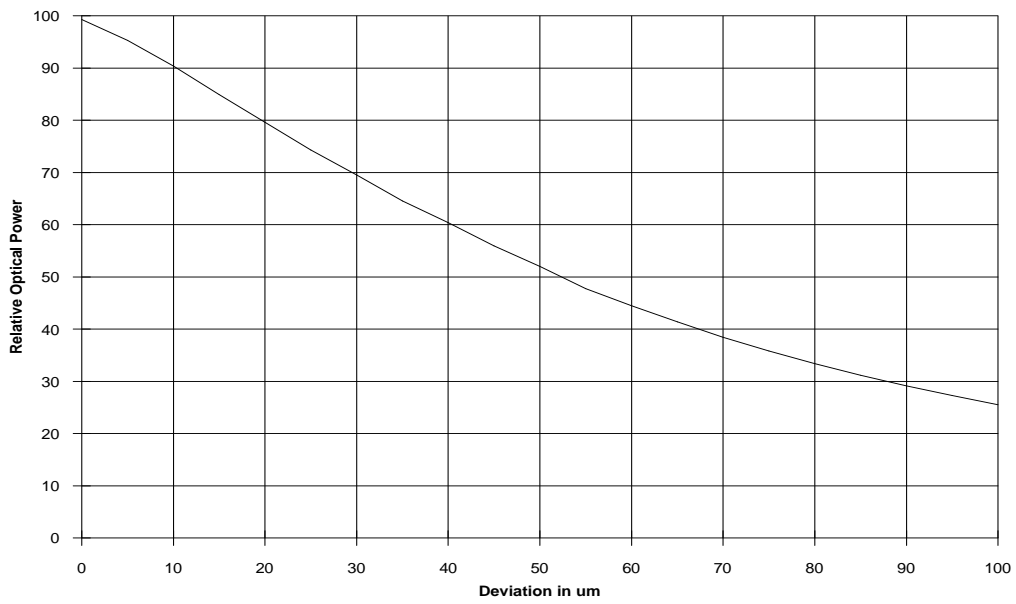


Figure 10: *Optical output power versus axial displacement along the diode emitting axis with respect to the LED window location*

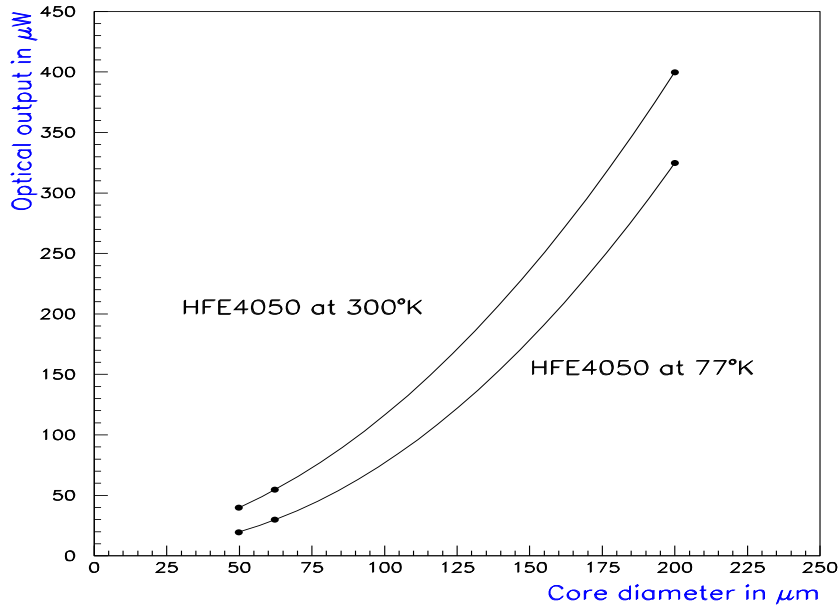


Figure 12: Output power at 30 mA input current as a function of the core diameter of the fibre for the HFE4050 diode

HFE4050, outputs a rod-like beam profile whereas a diode with two lenses (one collimating and one focalising), such as the ABB HAFO diodes, has a focal point ahead of the diode. In the latter case the point of maximum coupling is situated a few millimeters from the outermost lens, thus making it easier to obtain an optimal power coupling. This is particularly advantageous in the case of small core diameter fibres, but it has the disadvantage to increase the cost.

The receivers and the emitters can be packaged in ST cases but with a lower coupling efficiency than if the fibre is directly glued close to the lens (in the case of an emitter equipped with one lens, such as the HFE4050 diode). The effect of spatial positioning was studied with a diode mounted on a precise $XYZ\theta\phi$ positioning system in front of a coupling fibre, and the optical power output at the end of the fibre was measured in static mode with a light power meter. In figures 9 and 10 are displayed the variation of the coupling as a function of radial and axial displacements of a HFE4050 diode. The output power decreases with increased axial distance between emitter and fibre, suggesting that the fibre should be glued as close as possible to the emitter. To achieve a 95% efficient light coupling the spatial position of the fibre has to be precise to roughly 3 μm radially and to 5 μm axially.

The gluing of the fibre to the LED can be performed using the same method of positioning and light monitoring as already described. For the prototype, a TO46 (industrial standard) packaged diode was plugged, with lateral freedom, into a small aluminium case, as shown in figure 11. Then, the fibre was pushed into a 300 μm hole drilled at the centre of the case. The relative position of the emitting surface of the diode with respect to the fibre was adjusted to get the maximum output power. Finally, the package and the fibre were fixed to the case with epoxy glue and the free fibre end was equipped with a ST connector. Connecting a fibre to a component is called "pigtailling". The advantages of such a method are good coupling and the relatively small size of the package, but it is time-consuming (the TO46 package need not be used, in principle, but it simplifies the operation). For a future large scale production, we will have to automatize the operation and preferably reduce

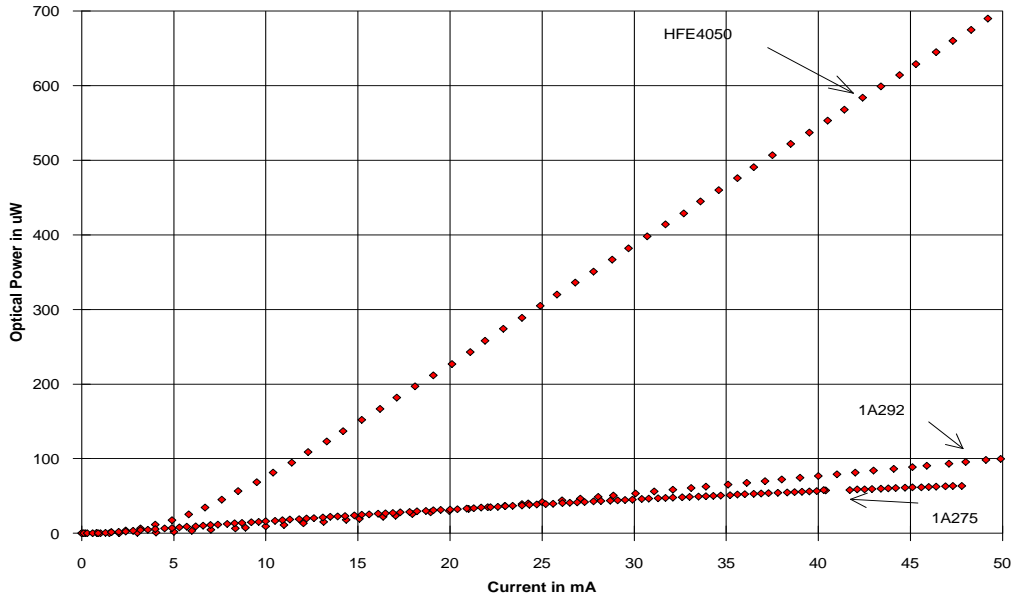


Figure 13: *Output optical power versus static input current for a few different diode types at room temperature*

the size of both the package and the connectors. We envisage using fibre ribbons that should be connected to the LEDs which preferably should be arranged in arrays integrated with the front-end electronics. A scheme for connecting ribbons onto a substrate has to be devised.

We have measured the amount of optical power that, from a given diode, can be coupled into a fibre as a function of its core diameter. A plot of these measurements is shown in figure 12 for the HFE4050 diode in static mode. It is clear that the optical power transmitted through the fibre scales with the size of its surface. Therefore, the need for high optical power coupled into the fibre motivates the use of a $200\ \mu\text{m}$ core size fibre for our analogue link. This point will be further developed in section 4.

Results similar to those obtained with the HFE4050 can be expected for other single ball lens diodes, whereas this may not be completely true for double-lens diodes such as the tested ABB HAFFO diodes, or for edge emitting diodes.

The numerical aperture of the fibre (defined as $\text{NA}=\sin(\theta_{max})$, with $2\theta_{max}$ the maximum emission divergence) is another factor affecting the amount of coupled light. However, for the HFE4050 diode the gain by choosing a large-NA fibre is small because of the collimation provided by the lens. Double-lens diodes, on the other hand, require using high-NA fibres to maximise the light output.

The optical output power from three different LEDs, using a standard ($200\ \mu\text{m}$, 0.22 NA) fibre, are shown in figure 13. The double-lens LED 1A292 is optimised for a fibre NA of 0.37, which explains the large difference between this LED and the HFE4050. (Note that even with a high-NA fibre the 1A292 outputs less power, although the difference is smaller). The third LED, 1A275, is a InP double-lens LED.

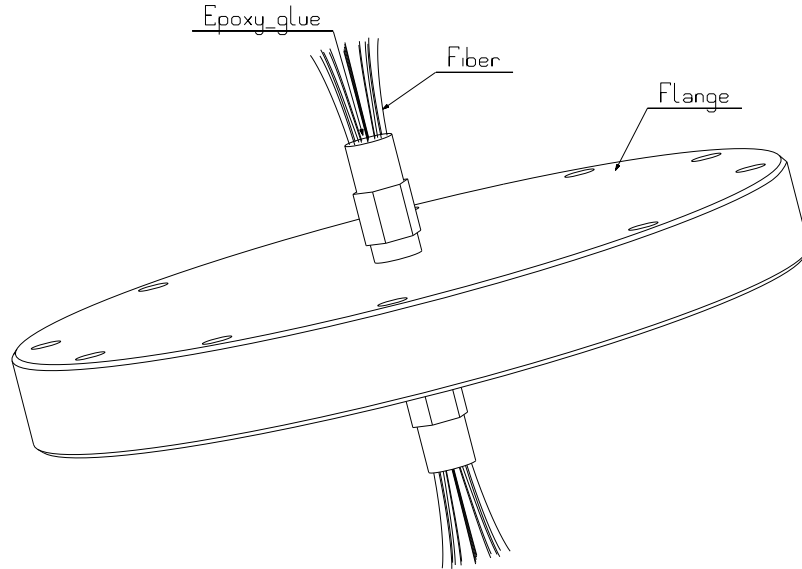


Figure 14: *Design of an optical feedthrough*

3.5 Feedthrough

A feedthrough is needed to bring the fibres out of the cryostat housing the liquid argon calorimeter. The design of the feedthrough developed for the test cryostat is shown in figure 14. The surface occupancy of the feedthrough is of the order of $0.1 \text{ mm}^2/\text{fibre}$ and up to 150 fibres can go through the flange, which is made of aluminium (easier to machine than stainless steel).

Two prototypes have been made with 40 and 128 fibres, respectively, glued into the hole with an epoxy resin (Stycast, suitable in cold environments). Both prototypes were tested in liquid nitrogen without showing any leakage (up to $10^{-9} \text{ torr}\cdot\text{l/s}$). One of the fibres was going in and out of the flange to study the transmission losses induced in a fibre by the feedthrough. No measurable effect was found.

The described feedthrough is usually called a warm feedthrough, since it is used for a cryostat where the feedthrough pipe is situated in an argon atmosphere above a liquid argon surface. In ATLAS, it is not yet decided if the optical feedthroughs will be warm or cold, meaning in direct contact with the liquid argon. This last case would possibly require a new design.

3.6 Light receiver

There are two main types of light receivers: Avalanche PhotoDiodes (APD) and PIN diodes. PINs are less sensitive than APDs to magnetic fields, radiation and temperature fluctuations. PIN diodes offer high quantum efficiency, low dark current and low operating voltage, making them easy to use. In addition, they are low cost. However, unlike APDs, they provide no amplification. Consequently, to cope with the losses caused by the various components of the link (pigtail, connectors, fibres), the PIN diode has to be connected to a transimpedance amplifier which converts the PIN current signal into a suitably large voltage signal.

We use a silicon PIN diode as receiver, being compatible with the wavelength of GaAs LEDs. An additional advantage of using silicon diodes is the prospects of integrating the receiver stage,

Parameter	Symbol	Min	Typ	Max	Units	Test Conditions
Peak response wavelength	λ_P		850		<i>nm</i>	
Flux responsivity $\lambda = 850nm$	R				<i>A/W</i>	
		0.45	0.6			50 μm , 0.20 NA fibre
			0.55			100 μm , 0.28 NA fibre
			0.55			200 μm , 0.40 NA fibre
Dark leakage current	I_D		0.05	2.0	<i>nA</i>	$V_R = 5V$
Reverse breakdown voltage	$B - VR$	110	250		<i>V</i>	$I_R = 10mA$
Response time	t_r				<i>ns</i>	1V prebias, 100mA peak
10-90%			17.0	30.0		$V_R = 5V$
10-90%			5.0	10.0		$V_R = 15V$
10-90%			1.0			$V_R = 90V$
Package Capacitance	C		1.4		<i>pF</i>	$V_R = 5V, f = 1MHz$
Field of View	F_oV		85		<i>Degrees</i>	

Table 2: Main characteristics of the HFD3002 diode for Honeywell data sheets

since there is much more experience in making silicon wafers than there is in using GaAs or other materials. PIN diode integration on silicon has already been done in industry.

The choice of PIN diode for the prototype was the HFD3002 (Honeywell) in ST packaging. In table 2, the main characteristics of the HFD3002 are shown. It is fast enough and has a low dark current. The quantum efficiency, or responsivity, is typically 0.5 mA/mW. PIN diodes exhibit linearity over more than four decades and the input noise is negligible compared to the noise of the front end electronics and of the transimpedance amplifier.

3.7 Transimpedance amplifier

The main parameters of the transimpedance amplifier are the equivalent input noise (EIN), the gain factor and the bandwidth.

For the prototype we used a transimpedance amplifier, made by the I.P.N. Lyon laboratory, called "FASTPAD" (based on a current conveyors concept (Icon)), whose circuit is shown in figure 15. The typical gain factor of this amplifier is 4000 V/A, its measured EIN is 10pA/ \sqrt{Hz} and it has a bandwidth of 30 MHz. The noise value is slightly too high to meet our requirements, but a new version with an EIN of 3pA/ \sqrt{Hz} will soon be delivered. Furthermore, a transimpedance amplifier with an EIN better than 1pA/ \sqrt{Hz} has been developed in the LAL laboratory in Orsay.

The linearity of the FASTPAD amplifier response has been measured with a pulse generator. As shown in figures 16 and 17 the dynamic response is linear to better than 2% over a range from 0 to 1.5 V output.

4 Prototype optical link

A 32-channel prototype of an analogue optical link was connected to a module of the RD3 preshower that was tested in particle beam in September of 1994. At the time of writing no final results are available from this test run, but preliminary data look promising. In this section we discuss the parameters of importance for the behaviour of the link, and some results are given from laboratory tests.

The front end electronics to which the prototype link was connected outputs a voltage from 0 to 2.5 V over a 50 Ω impedance. Thus, a driver was needed to convert this voltage into a forward current matched to the LED characteristics (bias point, dynamic impedance, gain). The driver had

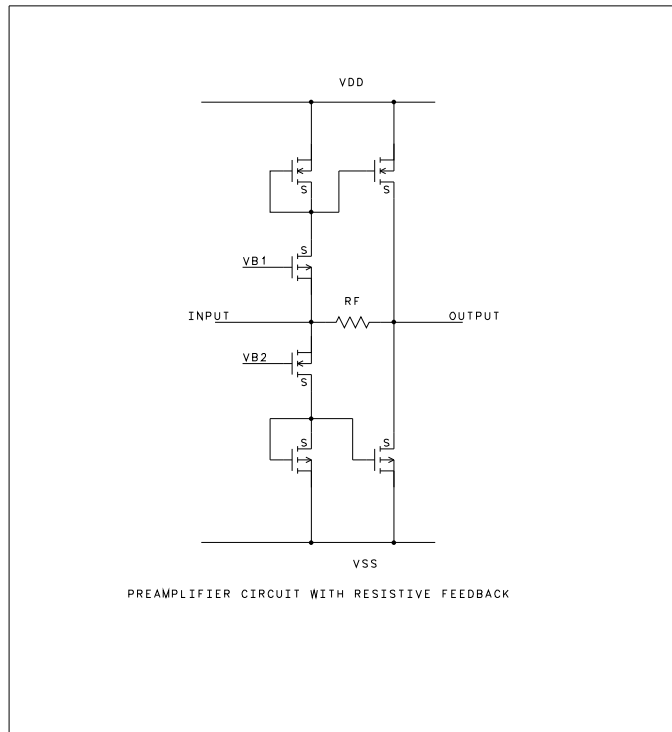


Figure 15: Scheme of a transimpedance amplifier

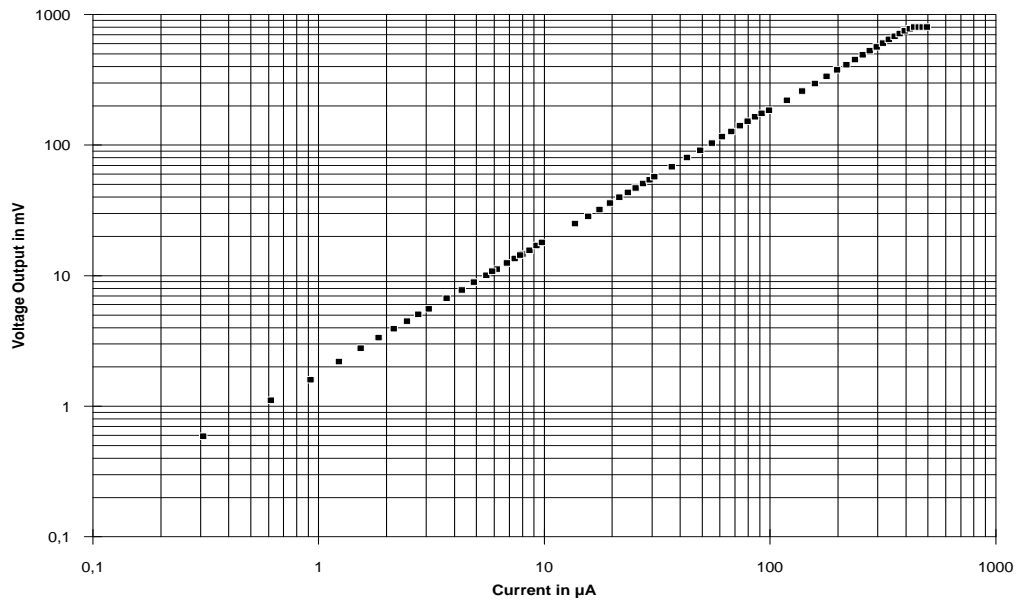


Figure 16: Dynamic range of the FASTPAD transimpedance amplifier

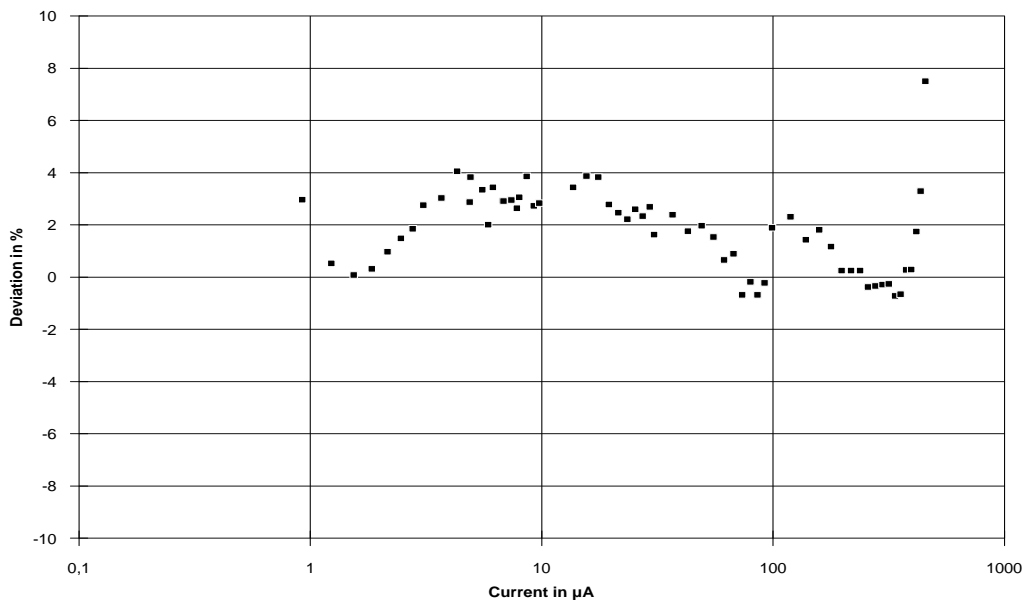


Figure 17: *Differential non-linearity of the FASTPAD transimpedance amplifier*

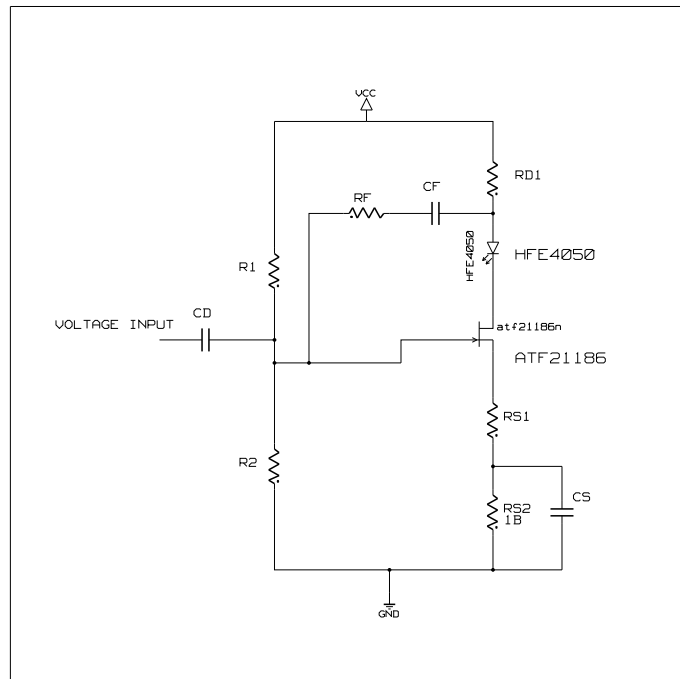


Figure 18: *Scheme of a LED driver*

to work in the cold and should not dissipate too much power. For LED lifetime considerations and to ease the design of such a driver, the signal current should not be too much over 50 mA. As a comparison, it is as difficult as building a voltage amplifier with a 2.5 V output over 50 Ω . We have built a driver that outputs 50 mA to the LED for a 2.5 V input voltage. The driver circuit is shown in figure 18. The EIN of such a system is negligible compared to the front end noise and was estimated to be below 100 μ V for a bandwidth of 50 MHz.

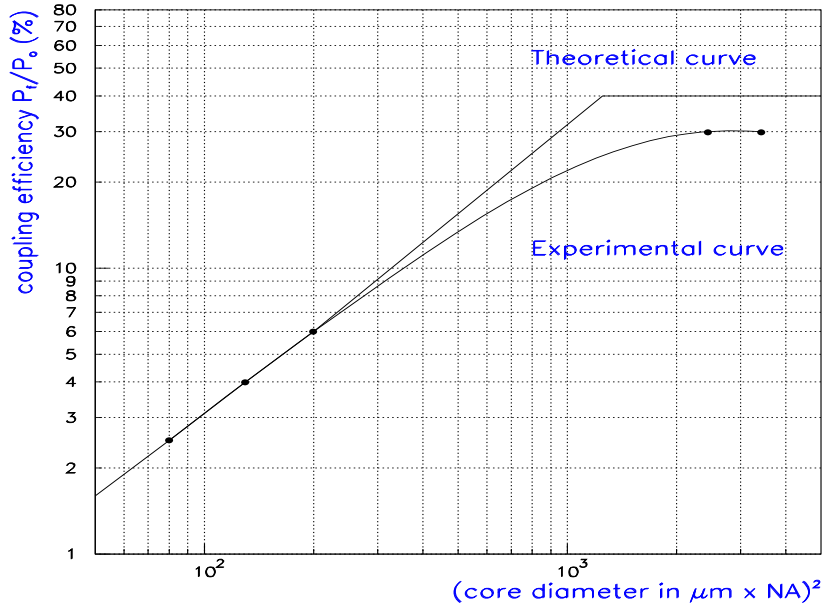


Figure 19: Typical efficiency of the coupling of the light power into various step index fibers and theoretical limit for this coupling for LED with a spherical lens (From Mitsubishi Electric)

In the future, the driver stage will be integrated into the front end electronics such that the front end output stage, which presently is a 50 Ω voltage buffer, becomes a current driver compatible with the chosen emitter.

As emitter we used a pigtailed HFE4050 LED connected to a 200/220/245 μm fibre (Cer-amOptec, optran UV, NA=0.22). Also four ABB HAFO 1A362 LEDs were included. Outside of the cryostat the fibre was connected to a HFD3002 PIN diode. All optical connectors were of the ST type. The noise of the LED as well as that of the PIN were negligible compared to the front end noise and the driver noise.

The PIN output current was fed into the FASTPAD transimpedance amplifier whose output was adjusted to 2.5 V full scale over a 50 Ω impedance.

The link bandwidth is roughly 30 MHz, limited by the current version of the transimpedance amplifier. The other components of the link have a bandwidth larger than 50 MHz. The parameters of importance for the behaviour of the link are the total equivalent input noise, the dynamic range and the linearity.

4.1 Equivalent input noise

The components of the optical link can be described by their "gain" characteristics:

Components	gain	equation	typical value	comments
Front end electronics	$G_{f.end}$	$V_{out} = G_{f.end}I_{in}$		
Driver	G_d	$I_{out} = G_dV_{in}$	0.02 mA/mV (S)	
LED	G_{LED}	$P_{out} = G_{LED}I_{in}$	0.04 mW/mA 0.06 mW/mA	Yield in the cold Yield in the warm
Connections	A_c	$P_{out} = A_cP_{in}$	1/4	mainly due to the pigtail- ing which induces a big loss, as shown in figure 19. The connection losses for the PIN diodes are negligi- ble in comparison.
Fibre	A_f	$P_{out} = A_fP_{in}$	0.99	for 10 metres which is negligible compared to the connections.
PIN diode	R_{PIN}	$I_{out} = R_{PIN}P_{in}$	0.5 mA/mW	Responsivity
Transimpedance	G_t	$V_{out} = G_tI_{in}$	4000 mV/mA (Ω)	

Using the above factorization, the transimpedance output voltage, V_{out} , can be expressed as a function of the driver input voltage, V_{in} :

$$V_{out} = G_t R_{PIN} A_f A_c G_{LED} G_d V_{in}, \quad (1)$$

or, in terms of current, the PIN diode output current, I_{out} , is related to the LED input current, I_{LED} , through the expression:

$$I_{out} = R_{PIN} A_f A_c G_{LED} I_{LED}, \quad (2)$$

which gives typically $I_{out} = (1/200)I_{LED}$.

The total noise is dominated by two sources – noise from the front end electronics, and noise from the transimpedance amplifier.

In order for the noise not to limit the performance of the link its contribution to the full noise must be small compared to the one given by the first stage noise (i.e. the noise already present at the output of the front end electronics). To be able to make a comparison, the two contributions must be evaluated equivalently in the chain, e.g. at the input of the transimpedance amplifier. At this location the gain of the first stage is divided by the loss of the link (typically 200).

To assure the dominance of the first stage noise, the additional noise introduced by the link should be at least three time smaller, thus causing an increase in the overall noise of less than 5%. We can express this by the following relation (using the fact that the link noise is essentially given by the transimpedance amplifier):

$$EIN_t \leq 0.3 R_{PIN} A_f A_c G_{LED} G_d G_{f.end} EIN_{f.end}. \quad (3)$$

To get an even better feeling for the importance of the different parameters affecting the total noise level, one can transform the above expression to the level of the LED:

$$EIN_t \leq 0.3 R_{PIN} A_f A_c G_{LED} EIN_{f.end/LED}, \quad (4)$$

where $EIN_{f.end/LED}$ is the noise of the front end at the LED level.

There are different ways to satisfy the above requirements, possible improvements are to:

- increase the driver gain. However, this will at the same time increase the maximum current driven into the LED in order to preserve the dynamic range. Thus it is not the best solution.

Figure 20: Power budget of the optical link

As an example, by assuming a 2.5 V full scale output from the front end electronics and a S_{max}/N ratio of 2500, one gets an output noise of 1 mV (over 50 Ω impedance). This leads to an $EIN_{f,LED}$ at the input of the LED of 20 μA and an $EIN_{f,endi}$ at the input of the transimpedance of 100 nA, to be compared to the EIN_i of 100 nA for the present transimpedance amplifier and to the 30 nA of the future amplifier. In the latter situation the front end noise is dominant.

4.2 Dynamic range and linearity

The dynamic range of the full system is linked to the noise level of the various components. However, restricting the non-linearity of the response from a component may at the same time limits its dynamic range and possibly that of the full system.

The equations in the previous section show that the S_{max}/N ratio is preserved through the link if the various components have a linear range that can handle this ratio. The maximum signal

level is adjusted with the driver gain to correspond to the full scale input current in the LED. Since the PIN diode can easily handle the dynamic range given by the front end, the "bottle neck" is the transimpedance amplifier. Its dynamic range has to be large enough and, as already pointed out, the noise should be three times smaller than that of the front end calculated at the same level.

The optical power budget of the full optical link is given in figure 20. One can clearly see the limitation from the transimpedance noise and the effects of the other components on the performances of the link.

The dynamic range of our prototype optical link was measured using a pulse generator as input to the LED driver and reading the transimpedance output voltage with a 12 bit ADC. A precision amplifier⁶⁾ was used to adapt the transimpedance signal to the best precision range of the ADC.

The resulting plot of output versus input voltage of the link is shown in figure 21. The noise of the system was measured to be below 1mV for a 30 MHz bandwidth. Thus, the dynamic range of the system was found to be at least 2000. A typical output signal before the transimpedance stage is shown in figure 22. The used FASTPAD transimpedance amplifier limited the bandwidth to 30 MHz.

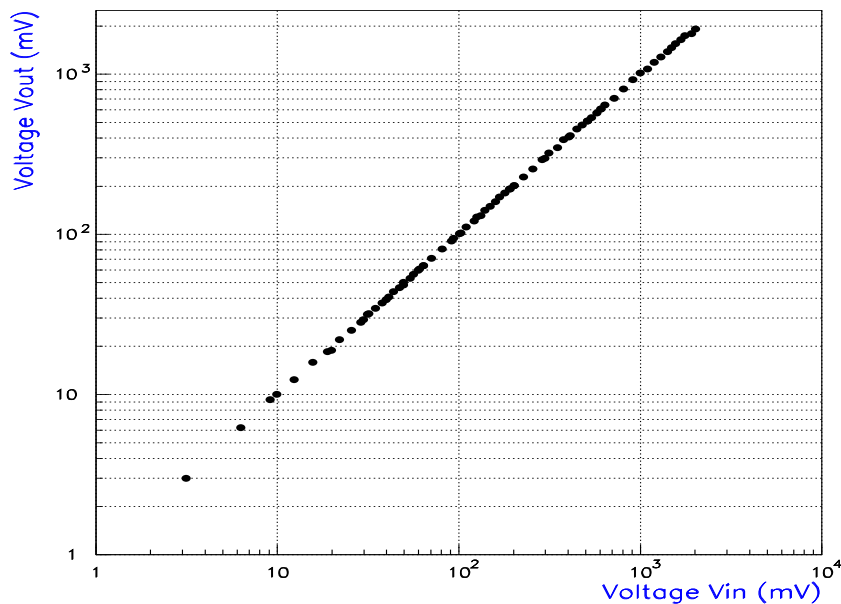


Figure 21: *Dynamic range of the full optical link, output voltage versus input voltage behaviour*

The non-linearity of the optical link response as a function of the input voltage is shown in figure 23. A $\pm 4\%$ non-linearity was achieved. As we have seen, restricting the non-linearity is equivalent to limiting the dynamic range.

For the LED it should be noted that the choice of current bias point affects the non-linearity, as can be seen in figure 7.

⁶⁾ Stanford research SR560

Figure 22: Typical output signal at the level of the PIN diode of the full optical link

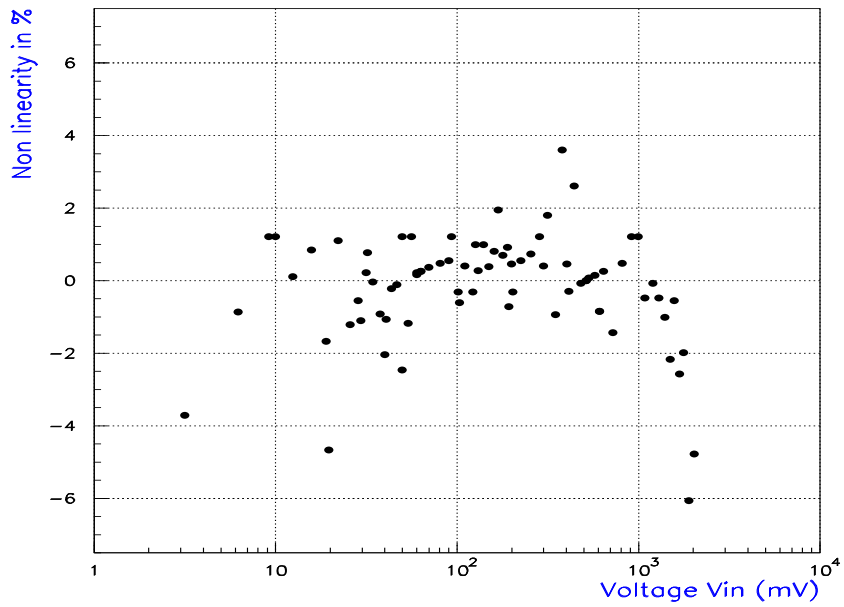


Figure 23: Differential non-linearity over the dynamic range of the optical link

5 Conclusions

We have shown the feasibility of an analogue optical link that can meet the requirements for the read-out of the presampler of the ATLAS liquid argon calorimeter. A dynamic range (S_{max}/N) of 2000 has been achieved and a value of 5000 seems possible in the future.

Further development work is going on, in the view of LHC, such as on the performance of LEDs, on the optical connections, on the transimpedance amplifier, on the integration of the various components, and on the radiation hardness of the system.

Soon we will have results on the performance of the 32 channels installed on the RD3 preshower which was tested at CERN in the combined ATLAS test run of September 1994. Preliminary results look promising.

A new test is planned for next year with a complete system, matching the LHC requirements, connected to a preshower prototype in a test beam.

References

- [1] B. Dinkespiler et al., ATLAS internal note LARG-NO-2, 1994.
- [2] P.M. Mooney and T.N. Theis, "The DX Center: A New Picture of Substitutional Donors in Compound Semiconductors", *Comments on Condensed Matter Physics*, vol 16, no 3, p 167, 1992.
- [3] M. Ettenberg et al. Linear, High-Speed, High-Power Strained Quantum-Well LED's, *IEEE Photonics tech. letters*, Vol 4,NO. 1, 1992.